UC Davis
UC Davis Previously Published Works

Title

Aldosterone activates the oncogenic signals ERK1/2 and STAT3 via redox-regulated mechanisms

Permalink

https://escholarship.org/uc/item/08j787dp

Journal

Molecular Carcinogenesis, 56(8)

ISSN

0899-1987

Authors

Queisser, Nina
Schupp, Nicole
Schwarz, Eva
et al.

Publication Date

2017-08-01

DOI

10.1002/mc.22643

Peer reviewed

RESEARCH ARTICLE

WILEY Molecular Carcinogenesis

Aldosterone activates the oncogenic signals ERK1/2 and STAT3 via redox-regulated mechanisms

Nina Queisser[1,2] | Nicole Schupp[1] | Eva Schwarz[1] | Christina Hartmann[1] |
Gerardo G. Mackenzie[2] | Patricia I. Oteiza[2,3] (iD)

[1] Institute of Toxicology, Medical Faculty, University of Düsseldorf, Düsseldorf, Germany

[2] Department of Nutrition, University of California, Davis, California

[3] Department of Environmental Toxicology, University of California, Davis, California

Correspondence
Patricia I. Oteiza, PhD, Departments of Nutrition and Environmental Toxicology, University of California, One Shields Avenue, Davis, CA 95616.
Email: poteiza@ucdavis.edu

Epidemiological studies found an increased risk for kidney cancer in hypertensive patients, of which a subgroup has high aldosterone (Ald) levels. We recently showed that Ald is genotoxic both in kidney tubular cells and in rats with mineralocorticoid-mediated hypertension. The present work investigated in vitro and in vivo, if the oxidative stress-mediated activation of the ERK1/2 pathway, and its downstream target STAT3, could be one mechanism involved in the potential oncogenic capability of excess Ald exposure. The effects of excess Ald were investigated in LLC-PK1 cells and in Ald-induced hypertensive rats. Ald caused cRaf, MEK1/2, and ERK1/2 phosphorylation both in LLC-PK1 cells and in rat kidneys. ERK1/2 activation led to an increased phosphorylation of MSK1, p90RSK, and STAT3. The involvement of ERK1/2 in the activation of STAT3 was evidenced by the capacity of the MEK inhibitor U0126 to prevent Ald-mediated ERK1/2 and STAT3 phosphorylation. Both in vitro and in vivo, the activation of ERK1/2 and STAT3 by Ald was dependent on the mineralocorticoid receptor and was triggered by an increase in cellular oxidants. Ald-mediated oxidant increase was in part due to the activation of the enzymes NADPH oxidase and NO synthase. Proliferation was significantly enhanced and apoptosis decreased in Ald-treated rat kidneys and/or LLC-PK1 cells. Results support the concept that the oxidant-mediated long-term activation of ERK1/2/STAT3 by persistently high Ald levels could trigger proliferative and prosurvival events. Ald-mediated promotion of cell survival and DNA damage could result in kidney cell transformation and initiation of cancer in hypertensive patients with hyperaldosteronism.

KEYWORDS
aldosterone, ERK1/2, kidney cancer, oxidative stress, STAT3

1 | INTRODUCTION

The mineralocorticoid aldosterone (Ald) plays a major role in the maintenance of electrolyte and fluid balance and in regulating blood pressure homeostasis. This is achieved through genomic actions of Ald via the mineralocorticoid receptor (MR). Ald mediates rapid, non-genomic effects, including the activation of NADPH oxidases.[1] On the other hand, we recently showed that excess Ald is genotoxic and causes oxidative stress in renal tubular cells[2,3] and in rat kidneys.[4–6] In hypertensive patients, epidemiological studies revealed higher cancer mortality and an increased risk to develop kidney cancer.[7–11] Proposed underlying factors are the mitogenic effects of the blood

pressure-regulating hormones angiotensin II and Ald. Abnormalities in apoptotic and proliferative processes associated with hypertension could lead to cellular overgrowth.

The mitogen-activated protein kinase (MAPK) pathway is an important signaling cascade that responds to extracellular stimuli like mitogens, hormones, or neurotransmitters, and has been implicated in the deleterious effects of excess Ald.[12,13] The highly specific cascade Raf/MEK/extracellular signal-regulated kinase (ERK) consists of the Ser/Thr kinase Raf, the highly homologous dual-specificity kinases MEK1/2, and the ubiquitously expressed ERK1/2.[14] Raf phosphorylation and the subsequent activation of MEK1/2 culminates in the activation of ERK1/2. MEK1 and MEK2 are the only commonly accepted downstream substrates of Raf[15,16] and ERK1/2 is the only identified substrate of MEK1/2.[17] Activated ERK1/2 catalyzes the phosphorylation of numerous substrate proteins including transcription factors, protein kinases, and phosphatases.[14] In fact, ERK1/2 has more than 50 identified substrates.[18]

Therefore, this cascade participates in the regulation of a large variety of processes, including cell cycle progression, cell survival, cell proliferation, migration, adhesion, differentiation, metabolism, and transcription.[14] It is not surprising that an abnormal activation of the ERK1/2 pathway can lead to cancer. Numerous solid tumors are known to express constitutive levels of phosphorylated ERK1/2, and the ERK1/2 pathway has been validated as target for novel anticancer therapies.[19] The constitutive activation of MEK1/2 has been also shown to result in cellular transformation.[20]

A key target of ERK1/2 is the transcription factor signal transducer and activator of transcription 3 (STAT3), which plays major roles in oncogenesis. The STAT proteins are activated by a series of extracellular signaling proteins such as growth factors and hormones, and they are involved in the regulation of physiological processes such as proliferation, apoptosis, and differentiation.[21] STAT3 is phosphorylated at specific serine/threonine residues, which is in part mediated by ERK1/2.[22,23] Normally, the activation of STAT3 is transient and under tight control, while its aberrant constitutive activation is associated with uncontrolled growth and cancer.[24] In particular, several studies have shown the activation of STAT3 in renal cell carcinomas.[25–27] Although STATs do not directly regulate cell cycle checkpoints or contribute to the repair of DNA damage, they promote tumorigenesis by deregulating signaling pathways directly involved in those processes.[28]

This work investigated both, in vitro and in vivo, the capacity of Ald to activate ERK1/2, and subsequently STAT3. The consequences of ERK/STAT3 activation on two central events in oncogenesis, resistance to apoptosis and increased cell proliferation were studied. Results show that excess Ald causes the oxidant-mediated activation of ERK1/2/STAT3 in association with abnormal apoptosis/proliferation rates in kidney cells. These findings support the concept that the oncogenic capacity of excess Ald is in part mediated through the activation of the ERK1/2/STAT3 signaling pathways.

2 | MATERIALS AND METHODS

2.1 | Materials

Epithelial porcine kidney cells with proximal tubular properties (LLC-PK1) were obtained from the American Type Culture Collection (Rockville, MA). Cell culture medium and reagents were obtained from PAA Laboratories GmbH (Pasching, Austria). The primary antibodies against phospho-(Tyr204)-ERK1/2 (sc-7383), ERK1/2 (sc-93), Bcl-x$_{S/L}$ (sc-634), and phospho-(Ser727)-STAT3 (sc-135649, used in Western blots and EMSAs) were obtained from Santa Cruz Biotechnology (Santa Cruz, CA). Phospho-(Ser338)-c-Raf (9427), c-Raf (9422), phospho-(Ser217/221)-MEK1/2 (9154), MEK1/2 (9122), phospho-(Thr581)-MSK1 (9595), MSK1 (3489), phospho-(Ser380)-p90RSK (9335), p90RSK (9355), phospho-(Ser727)-STAT3 (9134, used for immunohistochemistry), STAT3 (4904), and GAPDH (2118S) were purchased from Cell Signaling Technology Inc. (Beverly, MA). The antibody against Bak (ALX-210-002-R050) was obtained from Enzo Life Sciences (Lörrach, Germany), the one against PCNA (MAB424R)

from Merck Millipore (Schwalbach, Germany) and the one against α-tubulin (T6199) from Sigma-Aldrich (St. Louis, MO). The secondary antibody CF™488A donkey anti-rabbit IgG (20015) was purchased from Biotrend (Cologne, Germany). The CellTiter-Glo® Luminiscent Cell Viability assay, the oligonucleotides containing the consensus sequence for STAT3, and the reagents for the EMSA were obtained from Promega (Madison, WI). PVDF membranes were obtained from BIO-RAD (Hercules, CA) and Chroma Spin-10 columns from Clontech (Palo Alto, CA). The ECL plus Western blotting system was from Amersham Pharmacia Biotech Inc. (Piscataway, NJ). Apocynin (APO) was obtained from Calbiochem (San Diego, CA). Ald, eplerenone, L-nitroarginine methyl ester (L-NAME), tempol, U0126, and all other reagents were from the highest quality available and were purchased from Sigma-Aldrich. VAS2870 was kindly donated by Vasopharm BIOTECH GmbH (Würzburg, Germany).

3 | METHODS

3.1 | Cell culture

LLC-PK1 cells were cultured for 24 h in control medium, as described before.[3] Cells were subsequently treated with Ald (10 nM) for 0.5-24 h, depending on the assay. The concentration of Ald chosen is based on our previous studies,[2,3] and on its physiological relevance given that it is close to concentrations considered to have potential adverse renal effects in humans, but is low enough not to be cytotoxic.

3.2 | Animal treatment

Forty male Sprague-Dawley (RjHan:SD) rats (Janvier, Le Genest-St-Isle, France) were randomly divided into five groups at the age of 8 weeks (8 per group), and were equipped with osmotic minipumps (Alzet, model 2004; Durect Corporation, Cupertino, CA) under general anesthesia (ketamine 90 mg/kg and xylazine 6 mg/kg i.m.; medistar, Ascheberg, Germany). Group 2-5 received 0.75 μg Ald/h · kg body weight (BW) for 4 weeks via the osmotic minipump to induce a mineralocorticoid-dependent hypertension. Group 1 (control) received PBS via the osmotic minipump. Additionally, all animals got 1% (w/v) NaCl in the drinking water. Group 3 (spironolactone/ Ald) was additionally given 75 mg spironolactone/d · kg BW mixed in the food (ssniff, Soest, Germany), whereas group 4 (apocynin/Ald) and group 5 (L-NAME/Ald) were given 50 mg apocynin/d · kg BW or 25 mg L-NAME/d · kgBW via drinking water. Blood pressure was measured once a week noninvasively by the tail-cuff method (Visitech Systems, Apex, NY). To assess renal function at the beginning and at the end of the experiment, rats were placed in metabolic cages and urine samples were collected after 24 h.

After 4 weeks of treatment, animals were anesthesized (ketamine 120 mg/kg BW and xylazine 8 mg/kg BW i.m.; medistar, Ascheberg, Germany), the organs of the animals were perfused with ice-cold 0.9% (w/v) NaCl solution (Fresenius Kabi, Bad Homburg, Germany), and Deltadex 40 (AlleMan Pharma, Rimbach, Germany) containing 1% (w/v) procain hydrochloride (Steigerwald, Darmstadt, Germany), and the kidneys were excised. All animal experiments were performed in

accordance with the European Community guidelines for the use of experimental animals and with the German law for the protection of animals. The investigation conforms to the "Guide for the Care and Use of Laboratory Animals" published by the US National Institutes of Health (NIH Publication No. 85-23, revised 1996). The protocol was approved by the Regierung von Unterfranken, Würzburg, Germany (Permit number 55.2-2531.01-75/12).

3.3 | Electrophoretic mobility shift assay (EMSA)

Nuclear fractions were isolated as previously described.[29] For the EMSA, the oligonucleotides containing the consensus sequence of STAT3 were end-labeled with $(\gamma\text{-}^{32}P)$-ATP using T4 polynucleotide kinase and purified using Chroma Spin-10 columns. Samples were incubated with the labeled oligonucleotide (20 000-30 000 cpm) for 20 min at room temperature in 1× binding buffer (5× binding buffer: 50 mM Tris-HCl buffer, pH 7.5, containing 20% (v/v) glycerol, 5 mM $MgCl_2$, 2.5 mM EDTA, 2.5 mM DTT, 250 mM NaCl, and 0.25 mg/mL poly[dI-dC]). The products were separated by electrophoresis in a 6% (w/v) non-denaturing polyacrylamide gel using 0.5× TBE (Tris/borate 45 mM, EDTA 1 mM) as the running buffer. The gels were dried and the radioactivity was quantified in a Phosphoimager 840 (Amersham Pharmacia Biotech. Inc., Piscataway, NJ).

3.4 | Western blot analysis

Nuclear and total cell fractions were isolated as previously described.[29] To prepare kidney protein extracts, one quarter of each rat kidney was minced under nitrogen, suspended in lysis buffer (50 mM TRIS, 150 mM NaCl, 1 mM EDTA, 0.25% [w/v] sodium deoxycholate and 1% [v/v] Nonidet p40), and finally centrifuged at 8000g at 4°C for 5 min. The supernatant was transferred to a new tube and protein concentration was measured.[30]

Approximately 50 µg protein were separated by reducing 10% (w/v) or 12.5% (w/v) SDS-PAGE and electroblotted to PVDF membranes. Membranes were blocked for 2 h in 5% (w/v) bovine serum albumin, incubated in the presence of the corresponding primary antibodies for phospho-ERK/ERK, phospho-cRaf/cRaf, phospho-MEK1/2/MEK1/2, phospho-p90RSK/p90RSK, and phospho-MSK1/MSK1, phospho-STAT3/STAT3, PCNA, Bcl-x$_{S/L}$, Bak (all 1:1000) overnight, α-tubulin (1:4000) for 90 min at 37°C, and GAPDH (1:2000) for 60 min at room temperature. After incubation for 90 min at room temperature in the presence of the secondary antibody (HRP-conjugated) (1:10 000 dilution) the conjugates were visualized by chemiluminescence detection in a Phosphoimager 840 (Amersham Pharmacia Biotech. Inc.).

3.5 | Nuclear abundance of phospho-STAT3 assessed by confocal microscopy

LLC-PK1 cells (0.3×10^5) were seeded in 6-well plates on cover slips and treated with test substances for 4 and 24 h. Cells were washed and fixed in ice cold methanol for 7 min. After blocking for 1 h in blocking solution (10% w/v BSA, 0.1% v/v Tween 20), cells were incubated with the primary phospho-STAT3 antibody (1:200) for 1 h at 37°C, washed and subsequently incubated with the CF™488A-labeled secondary antibody

(1:200) for 1 h at room temperature in the dark. Cells were washed, stained with DAPI for 20 min at room temperature and mounted with confocal matrix. Confocal images were obtained by measuring the fluorescence at 515 nm (λexc 488 nm) with a TCS SP5 laser scanning confocal microscope (Leica Microsystems GmbH, Wetzlar, Germany). Quantification was done by measuring gray values of 100 cells per treatment with ImageJ 1.40 g (http://rsb.info.nih.gov/ij/).[31]

3.6 | Cell viability assay

The effect of Ald on cell viability was determined using the CellTiter-Glo Luminescent Cell Viability Assay. Briefly, cells (5000 cells/well) were plated in 96-well plates and grown overnight. Cells were incubated in the absence or the presence of Ald 10 nM, U0126 10 µM, or both for 24 h.

3.7 | Determination of apoptotic cell death by Annexin V and propidium iodide dual staining

LLC-PK1 cells were treated with Ald 10 nM, U0126 10 µM, or both for 24 h and apoptotic cells measured by FACS as previously described.[32] Briefly, all cells (attached and suspended) were collected and stained with annexin V-FITC (100× dilution) and propidium iodide (PI) (0.5 µg/mL) for 15 min. Annexin V-FITC and PI fluorescence intensities were analyzed using a BD Biosciences FACSCalibur (San Jose, CA). Annexin V(+)/PI(−) cells are early apoptotic cells; annexin V(+)/PI(+) cells are late apoptotic cells; while Annexin V(−)/PI(+) cells are necrotic cells. Data were analyzed using CellQuest sotfware (Becton Dickinson).

3.8 | Determination of mitosis and apoptosis rates

To determine mitotic and apoptotic cells, the protocol for the micronucleus frequency assay was used.[2] Briefly, LLC-PK1 cells (0.35×10^5) were seeded the day before and cells were treated with test compounds for 4 and 24 h. After treatment, the medium was removed, cells were washed and fresh medium containing 3 µg/mL cytochalasin B was added. After 24 h, cells were harvested, applied onto glass slides by cytospin centrifugation and fixed in ice cold methanol. Before counting, cells were stained with Gel Green and mounted with DABCO for microscopy. Mitotic and apoptotic cells were visually identified due to mitotic stages and condensed chromatin, respectively, and were counted within 1000 cells on each of two slides at a 500-fold magnification.

3.9 | Immunohistochemistry (IHC)

3.9.1 | Detection of phosphorylated MEK1/2, ERK1/2, MSK1, p90RSK, and STAT3

Paraffin kidney sections (5 µm) were mounted on glass slides, heated at 60°C for 1 h and deparaffinized. The slides were put in a microwave and tissues boiled in citrate buffer (10 mM citric acid, 2 M NaOH) for 15 min. The sections were blocked in 5% (v/v) donkey serum for 1 h at room temperature, washed, and subsequently incubated with 3% (v/v) hydrogen peroxide for 15 min at room temperature. Sections were

washed and incubated with 0.001% (w/v) avidin and subsequently with 0.001% (w/v) biotin. Then, sections were incubated with the primary antibodies for phospho-MEK1/2, phospho-MSK1, phospho-p90RSK, or phospho-STAT3 (1:200 dilution) overnight at 4°C, and followed by 45 min incubation with the biotin-conjugated secondary antibody in a 1:200 dilution. For the detection of phospho-ERK1/2, an additional step was incorporated into the protocol: sections were incubated with streptavidin-HRP (1:100) for 30 min, followed by tyramide amplification (10 min, Tyramide Signal Amplification Biotin System, PerkinElmer, Waltham, MA) and another streptavidin-HRP incubation for 30 min. Then, sections were incubated with ABC reagent (Vectastain-Elite ABC Kit) for 30 min at room temperature, and incubated with diaminobenzidine (DAB) (Vector Laboratories, Servion, Switzerland) for 1-10 min. Slides were counterstained with hematoxylin, and mounted with Eukitt (Sigma-Aldrich). Pictures were taken with a Leica DM 750 microscope at 200-fold magnification, using a Leica ICC50 HD camera (Leica Microsystems GmbH, Wetzlar, Germany). The ratio of positive/negative nuclei or positive/negative tubules was assessed using the cell image analysis software CellProfiler[33] within eight visual fields or counted manually (MEK).

3.9.2 | Detection of PCNA

Paraffin kidney sections (5 μm) were mounted on glass slides and deparaffinized. Sections were incubated in methanol containing 1.2% (v/v) H_2O_2, washed with deionized water and blocked in goat serum for 15 min. Anti-proliferating cell nuclear antigen (PCNA) antibody (Millipore, MAB424R) was applied in a 1:400 dilution over night at 4°C, followed by a 45 min incubation with the biotin-conjugated secondary antibody in a 1:200 dilution. Visualization was done by a standard ABC-DAB protocol as described above. Pictures were taken with a Leica DM 750 microscope at 200-fold magnification, using a Leica ICC50 HD camera (Leica Microsystems GmbH, Wetzlar, Germany). The ratio of positive cells/negative cells was assessed by the cell image analysis software CellProfiler[33] within eight visual fields.

3.10 | TUNEL assay

The frequency of apoptotic cells was detected by the In Situ Cell Death Detection Kit Fluorescein (Roche, Mannheim, Germany) according to the manufacturer's instructions and as described before.[34] Analysis was conducted using an Olympus BX43 microscope with 200-fold magnification. Six visual fields were analyzed per condition with at least 1000 cells per field. The number of TUNEL positive cells was counted and related to the DAPI positive area (as calculated by Image J 1.48r).

3.11 | Statistics

To determine significances between the groups SPSS 21 (IBM, Somer) was used, performing one-way analysis of variance (ANOVA) with subsequent post hoc comparisons by Bonferroni, after ensuring normal distribution with the Shapiro-Wilk test. Non-normal distributed data were analyzed with the Kruskal-Wallis test. A P-value ≤0.05 was considered statistically significant. Values are given as mean ± SEM. All experiments were performed at least three times.

4 | RESULTS

4.1 | In vitro experiments

4.1.1 | Ald activates the ERK1/2 signaling pathway

The activation of the ERK1/2 signaling pathway by Ald was investigated in pig kidney LLC-PK1 cells, a proximal tubular cell line. Phosphorylation levels of Raf/MEK/ERK were measured by Western blot in cells treated with 10 nM Ald for 0.5-24 h. A significant increase in p(Ser338)-cRaf and p(Ser217/221)-MEK1/2 phosphorylation was observed starting at 0.5 h, lasting up to 4 h incubation (Fig. 1A,B). The phosphorylation of ERK1/2 at Tyr204 in total cell fractions was significantly increased from 2 to 24 h incubation with Ald (Fig. 1C).

To investigate whether the activated ERK1/2 translocates into the nucleus to phosphorylate nuclear substrates, nuclear fractions of Ald-treated cells were analyzed for ERK1/2, p90RSK, and MSK1 phosphorylation by Western blot. Results showed that ERK1/2 is activated by 10 nM Ald in the nucleus after 1 h incubation, reaching a maximum after 4 h (Fig. 1D). Ald also caused subsequent phosphorylation of the ERK1/2 downstream nuclear targets p(Ser380)-p90-RSK and p(Thr581)-MSK1 (Fig. 1E,F).

4.1.2 | Ald activates STAT3

Transcription factor STAT3 is phosphorylated by ERK1/2 at serine 727 (Ser727). To investigate whether Ald activates this transcription factor in LLC-PK1 cells, the STAT3-DNA binding in nuclear fractions was evaluated by EMSA. In LLC-PK1 cells, the activation of STAT3, evaluated as nuclear STAT3-DNA binding by EMSA, was dependent on Ald concentration (5-100 nM). Significance was reached at 10 nM Ald (Fig. 2A). The maximum of STAT3-DNA binding was reached after 4 h incubation with 10 nM Ald (Fig. 2B). A significant increase in STAT3 Ser727 phosphorylation was also observed by Western blot within 1 and 24 h incubation with 10 nM Ald (Fig. 2C).

4.1.3 | Ald-induced ERK1/2 activation is responsible for STAT3 activation

Given that STAT3 can be also activated by other pathways, the specific activation by ERK1/2 was investigated using an inhibitor of the ERK1/2 signaling pathway. The effects of the MEK1/2 inhibitor U0126 on STAT3 activation was assessed by EMSA and immunostaining. When assessing STAT3 activation, U0126 inhibited Ald-mediated increase in STAT3-DNA binding (EMSA) (Fig. 3A). Furthermore, immunofluorescence staining revealed that after 4 and 24 h of treatment with 10 nM Ald, p-STAT3 nuclear abundance was significantly increased by Ald, which was prevented by simultaneously treating the cells with U0126 (Fig. 3B,D). All the above results demonstrate that ERK1/2 is in part responsible for the activation of STAT3 in Ald-treated cells.
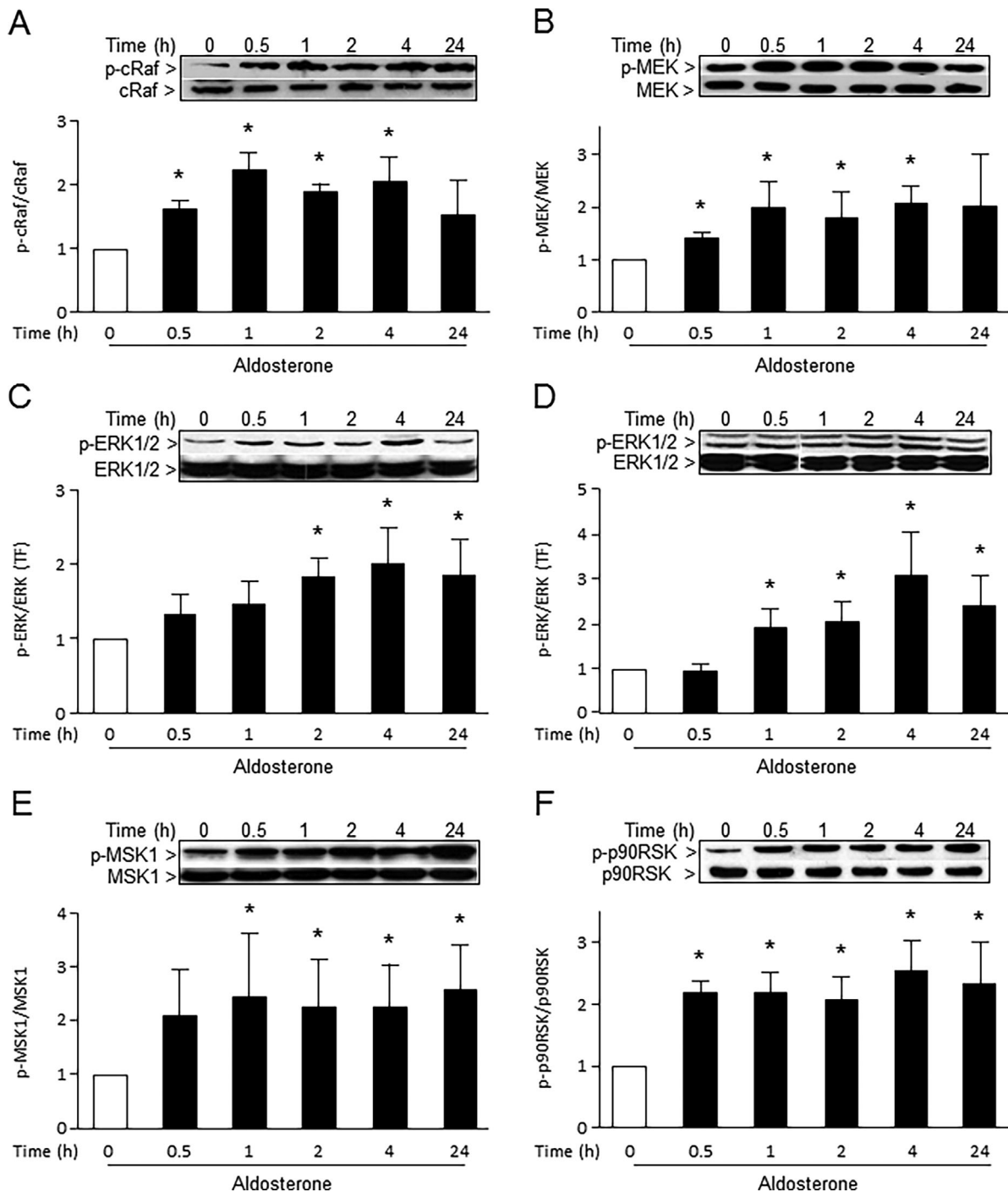
FIGURE 1 Ald promotes the activation of the ERK1/2 signaling pathway in LLC-PK1 cells in vitro. The activation of different events in the ERK1/2 signaling pathway was assessed by Western blot in (A-C) total cell and (D-F) nuclear fractions from LLC-PK1 cells treated with 10 nM Ald for 4 h. (A) p(Ser338)-c-Raf, (B) p(Ser217/221)-MEK1/2, (C and D) p(Tyr204)-ERK1/2, (E) p(Thr581)-MSK1, and (F) p(Ser380)-p90RSK. Representative images and the quantification of the bands are depicted. Results are shown as mean ± SEM. *$P \leq 0.05$ versus time point 0

4.1.4 | The MR, NAD(P)H oxidase, nitric oxide (NO) synthase (NOS), and cellular oxidants are involved in Ald-induced activation of ERK1/2 and the subsequent activation of STAT3

To investigate if the Ald-triggered activation of ERK1/2 and STAT3 is mediated via the MR, the effects of the MR antagonist eplerenone were assessed. Ald-mediated ERK1/2 activation and the subsequent activation of STAT3 were both significantly reduced by eplerenone (Fig. 4A,B). To

investigate the hypothesis that ERK1/2 activation and the subsequent activation of STAT3 occurred as a consequence of increased cellular oxidants, the influence of the cell permeant antioxidant tempol was investigated. Ald-induced activation of ERK1/2 and STAT3 was prevented by the simultaneous incubation of LLC-PK1 cells with tempol (Fig. 4C,D). These findings suggested that Ald-induced ERK1/2 activation and subsequent activation of STAT3 occurs through an increase in the
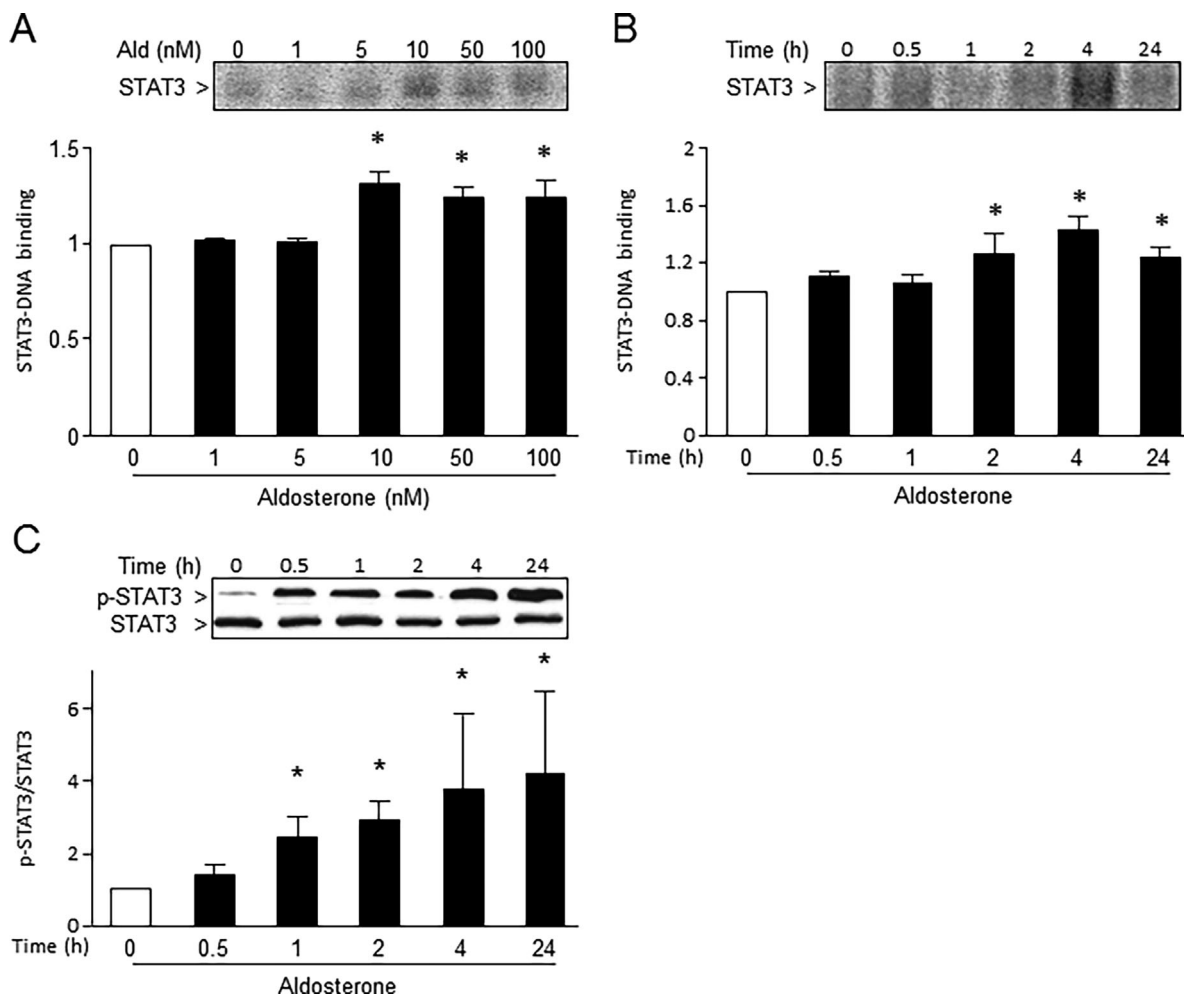
FIGURE 2 Ald promotes the activation of STAT3 in LLC-PK1 cells in vitro. (A) Concentration-dependency of STAT3 activation. STAT3-DNA binding was measured by EMSA in nuclear fractions, incubated in the absence (0), and presence of the indicated Ald concentrations for 4 h. (B) Kinetics of Ald (10 nM) induced STAT3-DNA binding in nuclear fractions as measured by EMSA. (C) The nuclear presence of p(Ser727)-STAT3 was evaluated by Western blot in LLC-PK1 cell nuclear fractions that were incubated with 10 nM Ald for the indicated time points. Representative images and the quantification of the bands are depicted. Results are shown as mean ± SEM. *$P \leq 0.05$ versus control

cellular production of oxidants, especially $O_2^{\cdot-}$. To further investigate the mechanisms involved in the activation of ERK1/2 and STAT3, LLC-PK1 cells were incubated for 4 h with or without Ald and simultaneously treated with the NAD(P)H oxidase inhibitor VAS, and with the NOS inhibitor L-NAME. VAS and L-NAME caused a significant inhibition of ERK1/2 and STAT3 activation as determined by Western blot and EMSA, respectively (Fig. 4C,D).

4.1.5 | Ald-mediated activation of ERK1/2 leads to increased cell proliferation

Since cellular overgrowth characterizes the development of cancer, cell proliferation was analyzed in Ald-treated LLC-PK1 cells. First, mitotic rates were measured. A significant increase of mitotic rates was observed after treating the cells with Ald for 4 and 24 h. A significant reduction of the mitotic rate was found when cells were simultaneously incubated with the MEK inhibitor U0126 (Fig. 5A,B). Consistently, at 24 h of treatment, U0126 significantly reduced cell growth by 55% as determined using the CellTiter-Glo Luminiscent Cell

Viability Assay. Although Ald did not affect cell viability, it acted attenuating the decrease in cell viability caused by U0126 (Fig. 5C). We next investigated the expression of PCNA, a protein which is found in the cell nucleus during the S-phase of the cell cycle. In agreement with the raised cell proliferation of Ald-treated cells, PCNA protein levels measured by Western blot were significantly increased in Ald-treated cells within 0.5 and 24 h of incubation (Fig. 5D).

4.1.6 | Ald-mediated activation of ERK1/2 leads to reduced apoptosis

Besides an enhanced cell proliferation, resistance to apoptosis plays an important role in the development of cancer. For this purpose, we evaluated, by Annexin V staining, the effect of Ald on phosphatidylserine externalization. The percent of annexin V(+) cells was not significantly different between Ald-treated and control groups. Treatment with U0126 significantly increased the number of annexin V(+) cells, while Ald partially attenuated the number of annexin V(+) cells induced by U0126 (Fig. 6A,B).
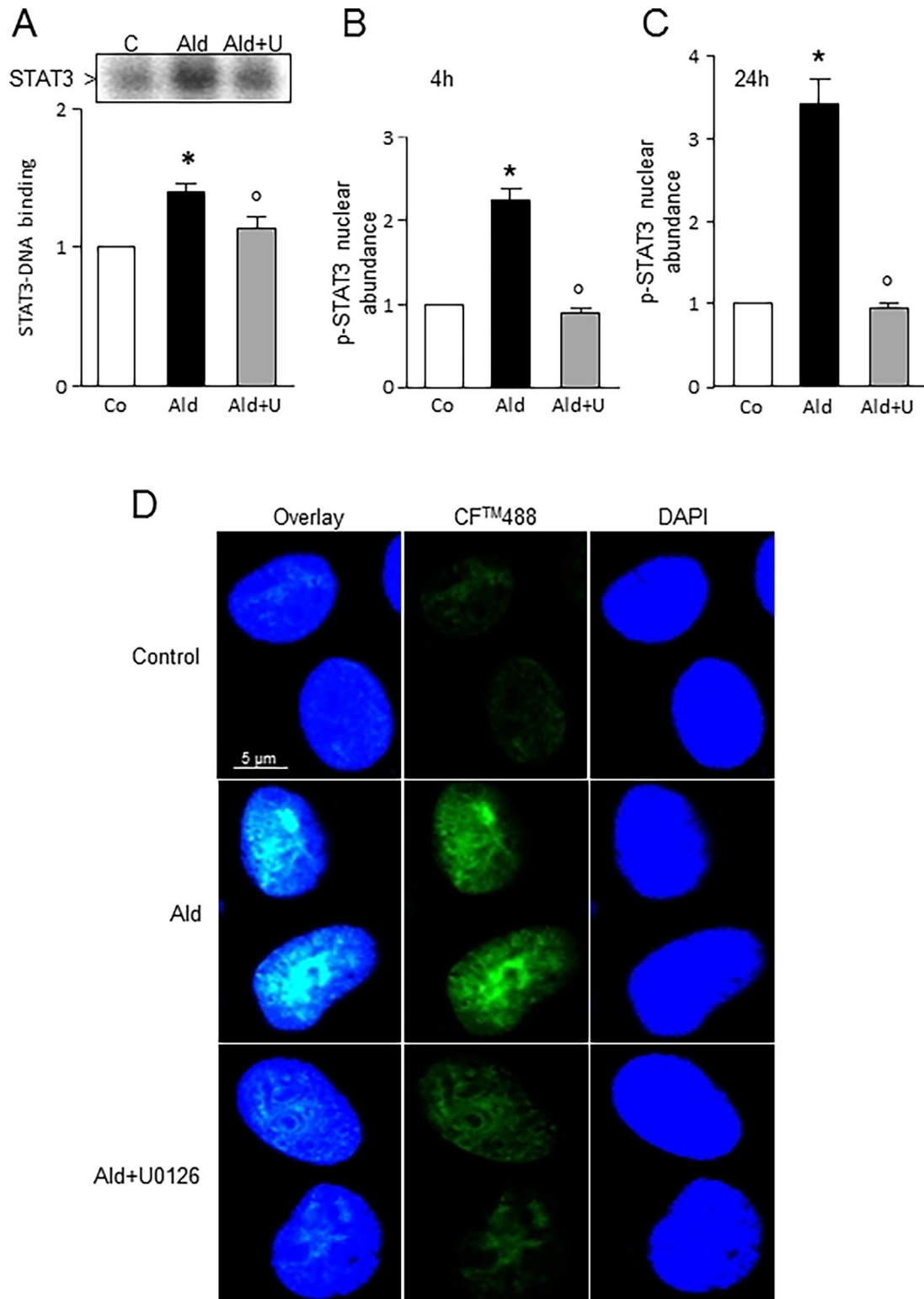
FIGURE 3 Inhibition of MEK1/2 activation prevents Ald-induced STAT3 activation. Ald-induced STAT3-DNA binding was blocked by using the MEK1/2 inhibitor U0126 (U; 10 μM) in LLC-PK1 cells treated with 10 nM Ald for 4 h (A) as assessed by EMSA. p(Ser727)-STAT3 nuclear abundance was assessed by immunostaining and confocal microscopy of LLC-PK1 cells treated for 4 h (B) or 24 h (C) with 10 nM Ald in the absence or presence of U0126 (U; 10 μM). Quantification of the fluorescence of all treatments was performed using Image J. (D) Representative images of cells stained for nuclear abundance of p(Ser727)-STAT3 after treatment with 10 nM aldosterone for 24 h. Results are shown as mean ± SEM. *$P \leq 0.05$ versus control (Co), °$P \leq 0.05$ versus Ald
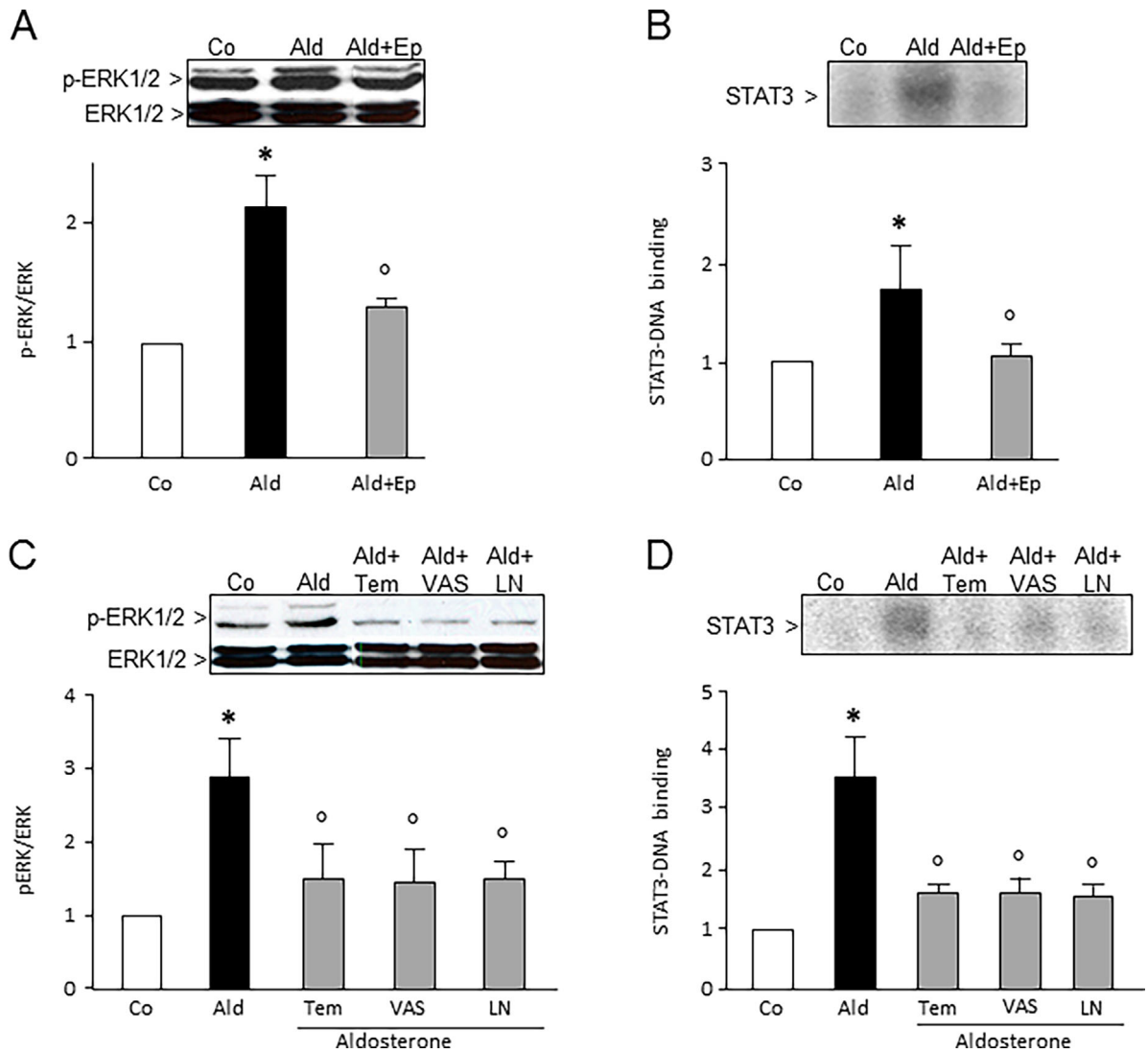
FIGURE 4 The MR, NADPH oxidase, and NOS are involved in Ald-induced activation of ERK1/2 and the subsequent activation of STAT3. (A and C) Western blots for p-ERK1/2 in total cell extracts from LLC-PK1 cells treated with 10 nM Ald for 4 h in the absence or the presence of (A) the MR antagonist eplerenone (Ep; 0.5 μM), and (C) the antioxidant tempol (Tem; 50 μM), the NADPH oxidase inhibitor VAS (VAS; 1 μM) and the NOS inhibitor L-NAME (LN; 50 μM). Representative images and the quantification of the bands are shown as the ratio of p(Tyr204)-ERK1/2/ERK. (B and D) STAT3-DNA binding in nuclear fractions was assessed by EMSA in LLC-PK1 cells treated with 10 nM Ald for 4 h in the absence or the presence of: (B) eplerenone (Ep; 0.5 μM) and (D) tempol (Tem; 50 μM), VAS (VAS; 1 μM), and L-NAME (LN; 50 μM). Representative images and the quantification of the bands are depicted. Results are shown as mean ± SEM. *$P \leq 0.05$ versus control (Co), ° $P \leq 0.05$ versus Ald

Apoptotic rates were also measured microscopically in cells treated with 10 nM Ald for 4 and 24 h, by gel green staining and subsequent microscopy. A significant reduction of apoptotic cells was observed in Ald-treated cells after 24 h incubation. The simultaneous treatment with Ald and U0126 not only prevented the reduction caused by Ald, but led to a two- to threefold increase in apoptotic rates (Fig. 6C,D).

Moreover, Western blots for the anti-apoptotic protein Bcl_{XL} and the pro-apoptotic proteins Bcl_{XS} and Bak were done in Ald-treated LLC-PK1 cells. A significant increase of the anti-apoptotic protein Bcl_{xL} was observed after 0.5, 2, 4, and 24 h incubation with 10 nM Ald (Fig. 6E), whereas a significant decrease of the pro-apoptotic proteins Bcl_{xs} and Bak was observed in Ald-treated cells after 4 and 24 h or 2-24 h, respectively (Fig. 6E).

4.2 | In vivo experiments

4.2.1 | Ald activates the ERK1/2 signaling pathway

To investigate if hyperaldosteronism also causes activation of the ERK1/2 signaling pathway in vivo, IHC analysis for p-ERK1/2 (Tyr204) was done in kidney cortex. A significant increase of p-ERK1/2-positive nuclei was found in renal cortex and medulla from Ald-treated rats, which was prevented/mitigated when simultaneously treated with spironolactone, apocynin and L-NAME (Fig. 7A,B). A similar pattern of effects on ERK1/2 phosphorylation was observed by Western blot in total kidney extracts (Fig. 7C).

The upstream MEK1/2 is located in the cytoplasm. IHC staining showed a significant increase of phospho-MEK1/2-positive tubules in the cortex and a significant reduction of the staining in the
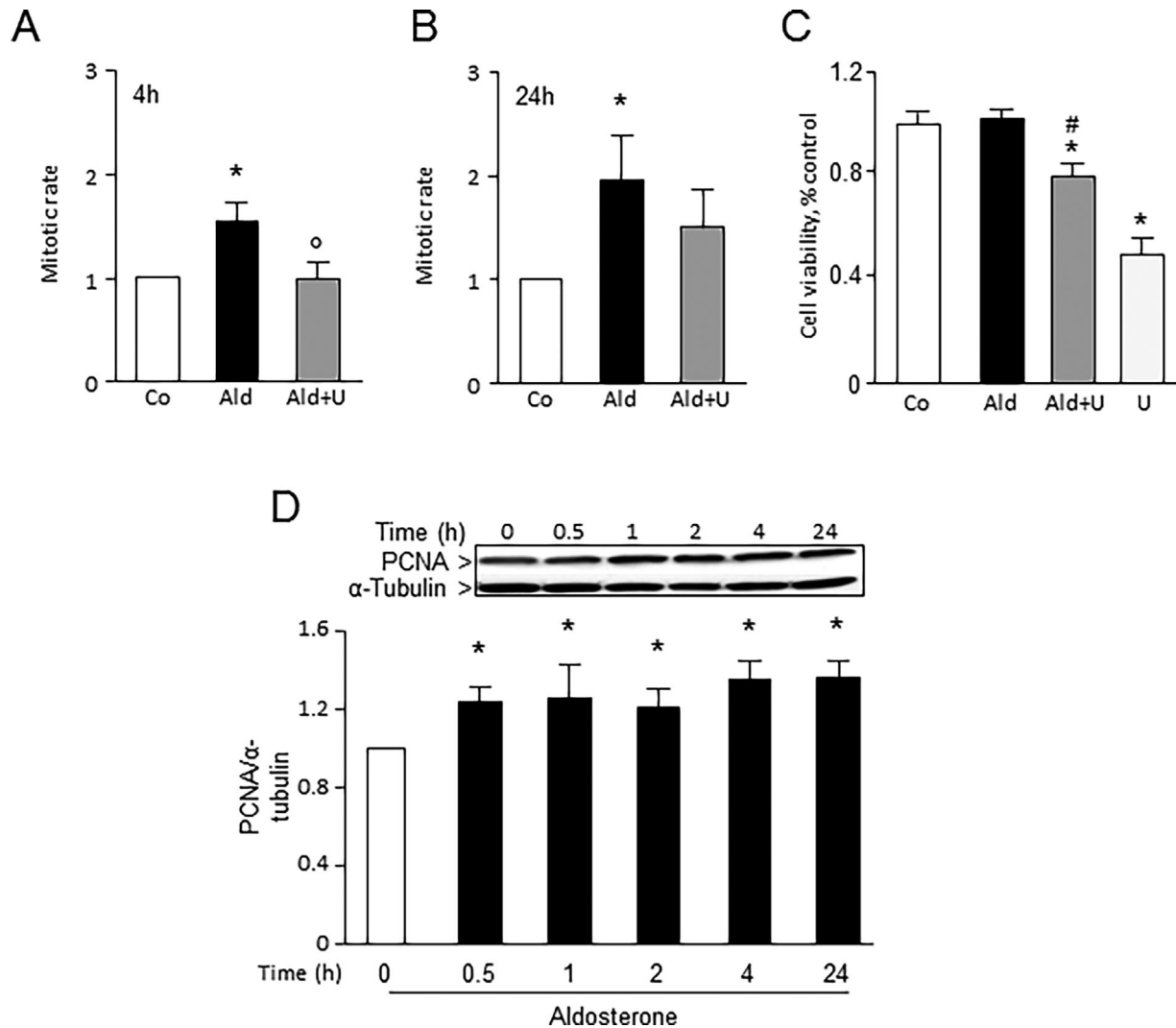
FIGURE 5 Ald-mediated activation of ERK1/2 and STAT3 leads to increased cell proliferation. (A and B) LLC-PK1 cells were incubated with or without 10 nM Ald, and with Ald in the presence of the MEK1/2 inhibitor U0126 (U; 10 μM) for 4 (A) and 24 h (B). Mitotic rates were quantified in microscopy images as described in the Methods section. (C) LLC-PK1 cells were incubated with or without 10 nM aldosterone (Ald), and with Ald in the absence or the presence of the MEK1/2 inhibitor U0126 (U; 10 μM) for 24 h. Cell viability was measured as described in Methods. Values are shown as means ± SEM. (D) Expression of PCNA was analyzed by Western blot in LLC-PK1 cells treated with 10 nM Ald for 4 h. Representative images and the quantification of the bands are shown. Results are shown as mean ± SEM. *$P \leq 0.05$ versus control (Co), °$P \leq 0.05$ versus Ald, #$P \leq 0.05$ versus U alone

apocynin/Ald and L-NAME/Ald groups (Fig. 8A,B). In the medulla the increase in MEK phosphorylation, although almost double that of the controls, was not statistically significant (Fig. 8B). Downstream of ERK1/2, MSK1 and 90RSK phosphorylation was assessed. pMSK1-positive nuclei were significantly higher in the renal cortex and medulla from the Ald-treated group compared to controls (Fig. 8A,C). A significant reduction of pMSK1-positive nuclei was observed in the apocynin/Ald group in cortex and medulla and in medulla from the L-NAME/Ald group (Fig. 8C). p-p90RSK-positive nuclei were more than three times higher in cortex and medulla in Ald-treated rat kidneys compared to controls, and a significant reduction of p-p90RSK-positive nuclei was found in the whole kidney from rats simultaneously treated with spironolactone, apocynin and L-NAME (Fig. 8D). Representative pictures are depicted in Fig. 8A.

4.2.2 | Ald activates STAT3 in vivo

The in vivo Ald-mediated phosphorylation of STAT3 at Ser727 was next investigated. IHC staining showed a significant increase of p-STAT3-positive nuclei in cortex and medulla of Ald-treated animals compared to controls, while a significant reduction of p-STAT3-positive nuclei was found in the rats treated simultaneously with spironolactone, apocynin and L-NAME in the cortex, but only with apocynin in the medulla (Fig. 8A,E).

4.2.3 | Ald-mediated ERK1/2/STAT3 activation modulates cell proliferation and apoptosis in vivo

In vivo cell proliferation was investigated by IHC for PCNA, a protein critical for DNA replication. A significant increase of PCNA-positive nuclei was observed in the renal cortex and
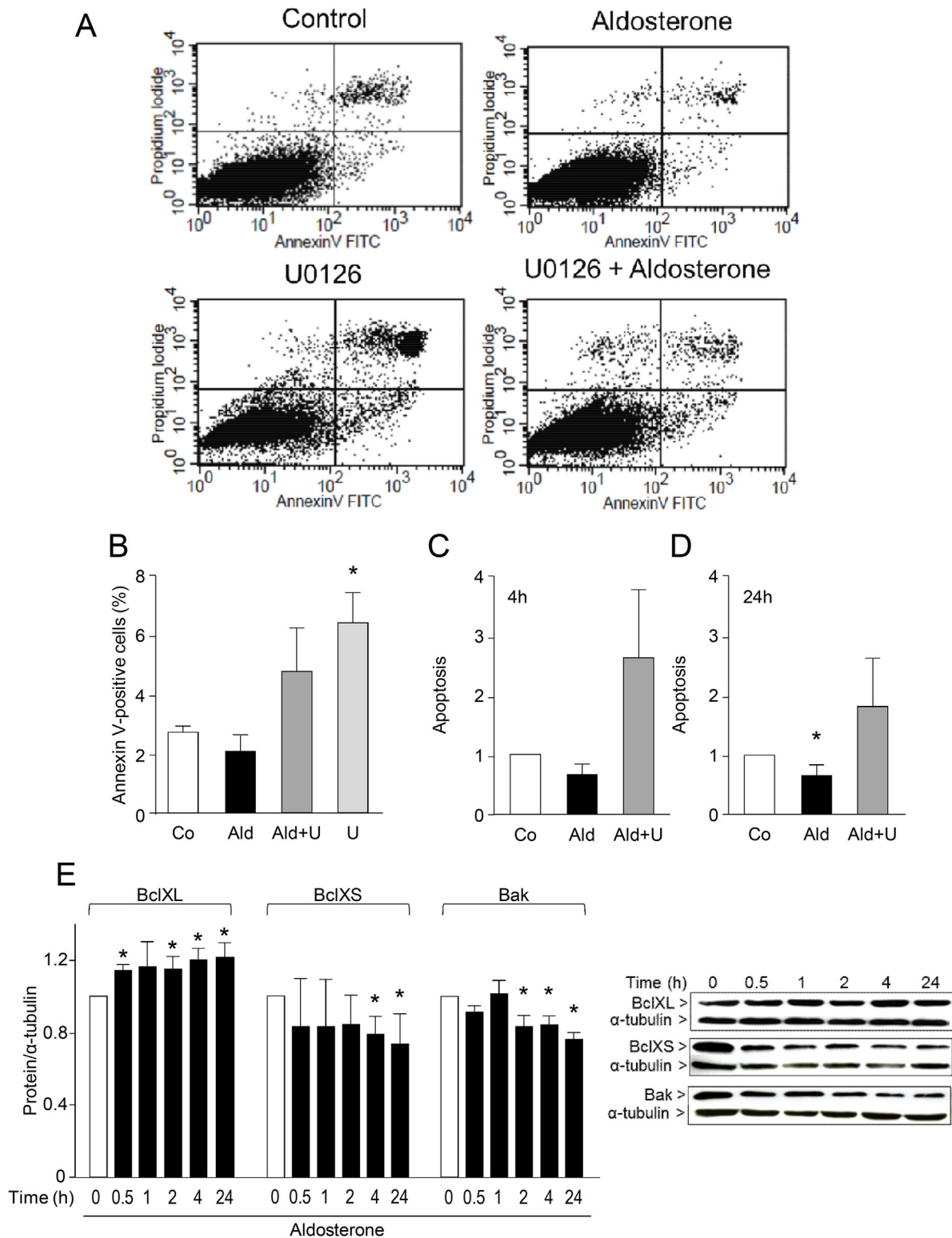
FIGURE 6 Ald-mediated activation of ERK1/2 and STAT3 leads to reduced apoptosis. (A) LLC-PK1 cells were incubated with or without 10 nM aldosterone (Ald), and with Ald in the absence or the presence of the MEK1/2 inhibitor U0126 (U; 10 μM) for 24 h. At 24 h, cells were stained with Annexin V/PI, and the percentage of apoptotic cells was determined by flow cytometry. Representative images are shown. (B) Results were quantified and expressed as percent of annexin V(+) cells. (C and D) LLC-PK1 cells were incubated with or without 10 nM Ald, and with Ald in the presence of the MEK1/2 inhibitor U0126 (U; 10 μM) for 4 and 24 h. Apoptotic cells were quantified in the microscopy images as described in the Methods section. (E) Expression of Bcl_{XL}, Bcl_{XS}, and Bak was analyzed by Western blot in LLC-PK1 cells treated with 10 nM Ald for 0-24 h. Representative images and the quantification of the bands are depicted. Results are shown as mean ± SEM. *$P \leq 0.05$ versus control (Co), °$P \leq 0.05$ versus Ald
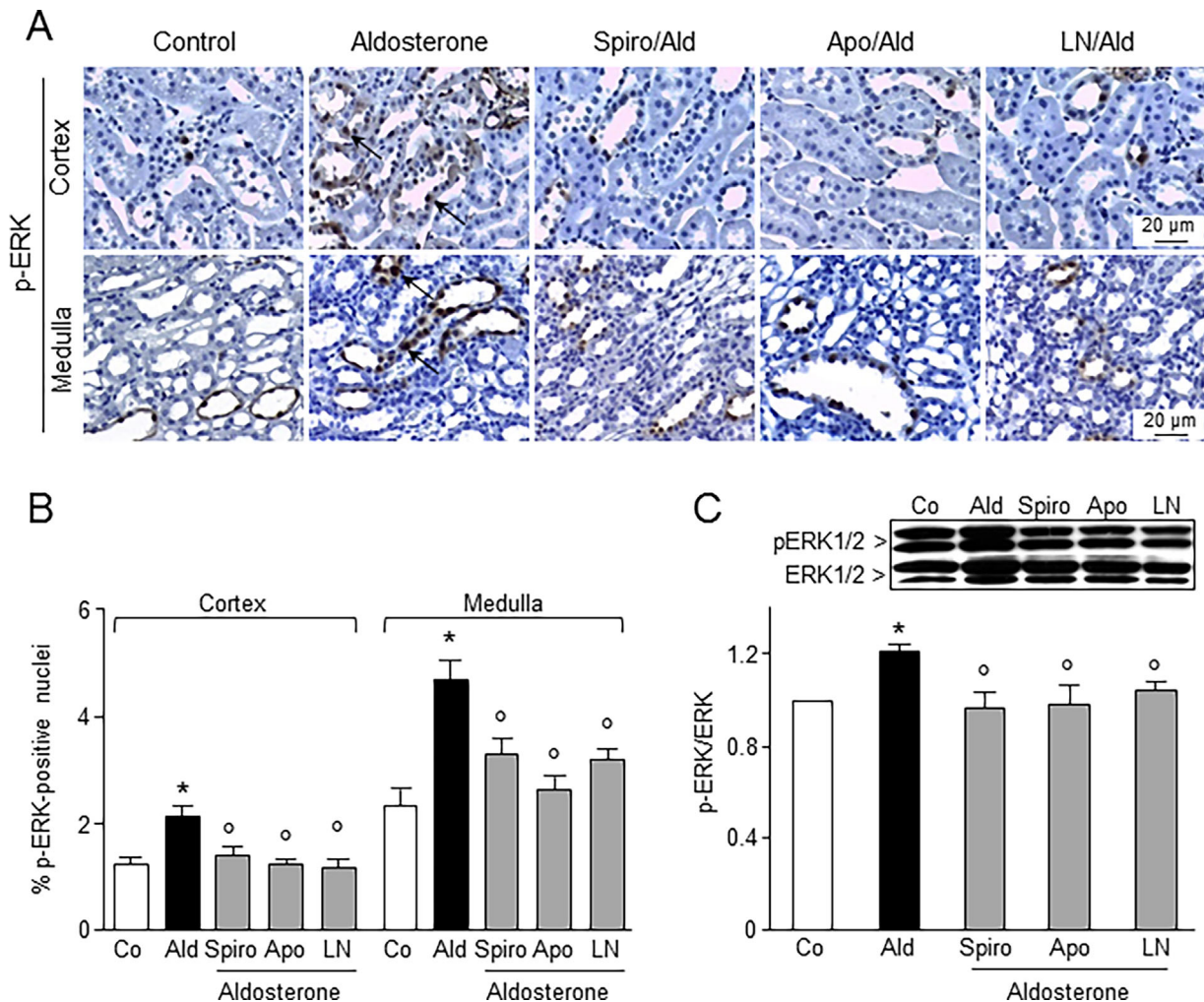
FIGURE 7 Ald activates the ERK1/2 signaling pathway in vivo. Rats were untreated (Control; Co) or treated for 4 weeks with aldosterone (Ald), and simultaneously with spironolactone (Spiro), apocynin (Apo), or L-NAME (LN). (A) Representative images for the IHC staining of phospho-(Tyr204)-ERK-positive nuclei from cortex and medulla are shown. Arrows highlight positive cells. (B) p(Tyr204)-ERK1/2-positive nuclei were quantified using the cell image analysis software CellProfiler[33] within eight visual fields. (C) p(Tyr204)-ERK1/2 and ERK levels measured by Western blot in rat kidney extracts. Representative images and the quantification of the bands are shown. Results are shown as mean ± SEM. *$P \leq 0.05$ versus control, °$P \leq 0.05$ versus Ald treatment

medulla from Ald-treated rats compared to controls. PCNA-positive nuclei were significantly lower in kidneys from rats treated simultaneously with Ald and spironolactone, apocynin or L-NAME (Fig. 9A,B).

Staining for apoptosis with the TUNEL assay did not show significant differences in the kidney (Fig. 9C). In the cortex, the amount of apoptotic cells of Ald-treated animals showed a trend ($P = 0.08$) for higher values than in controls. Spironolactone significantly reduced apoptosis in the cortex compared to Ald-treated animals and in the medulla compared to control animals.

The expression of the anti-apoptotic protein Bcl$_{XL}$ was significantly increased in total kidney extracts of the Ald-treated group whereas that of the pro-apoptotic protein Bcl$_{XS}$ was significantly decreased. No statistical differences were observed among Spironolactone-, apocynin-, and L-NAME-treated groups (Fig. 9D,E).

5 | DISCUSSION

This paper investigated if the Ras/Raf/MEK/ERK pathway and its downstream target, the STAT3 transcription factor, could contribute to kidney cell survival and proliferation when exposed to excess Ald. We found that both in vitro and in vivo, Ald promoted the activation of Ras/Raf/MEK/ERK and of STAT3, which was associated with increased cell mitosis and decreased apoptosis, central events in cancer promotion and development. In vivo and in vitro studies point to a major role of NADPH oxidase and NO synthase activation in the triggering of these oncogenic events by excess Ald.

Activation of the Ras/Raf/MEK/ERK pathway has key regulatory functions on cell proliferation, apoptosis and differentiation. ERK1/2 aberrant activation is associated with increased cell growth and oncogenesis.[35] As we currently observed for Ald in LLC-PK1 cells and rat kidney tubules, the MR-dependent activation of Raf, MEK1/2 and ERK1/2 was previously reported in smooth muscle cells, cardiac
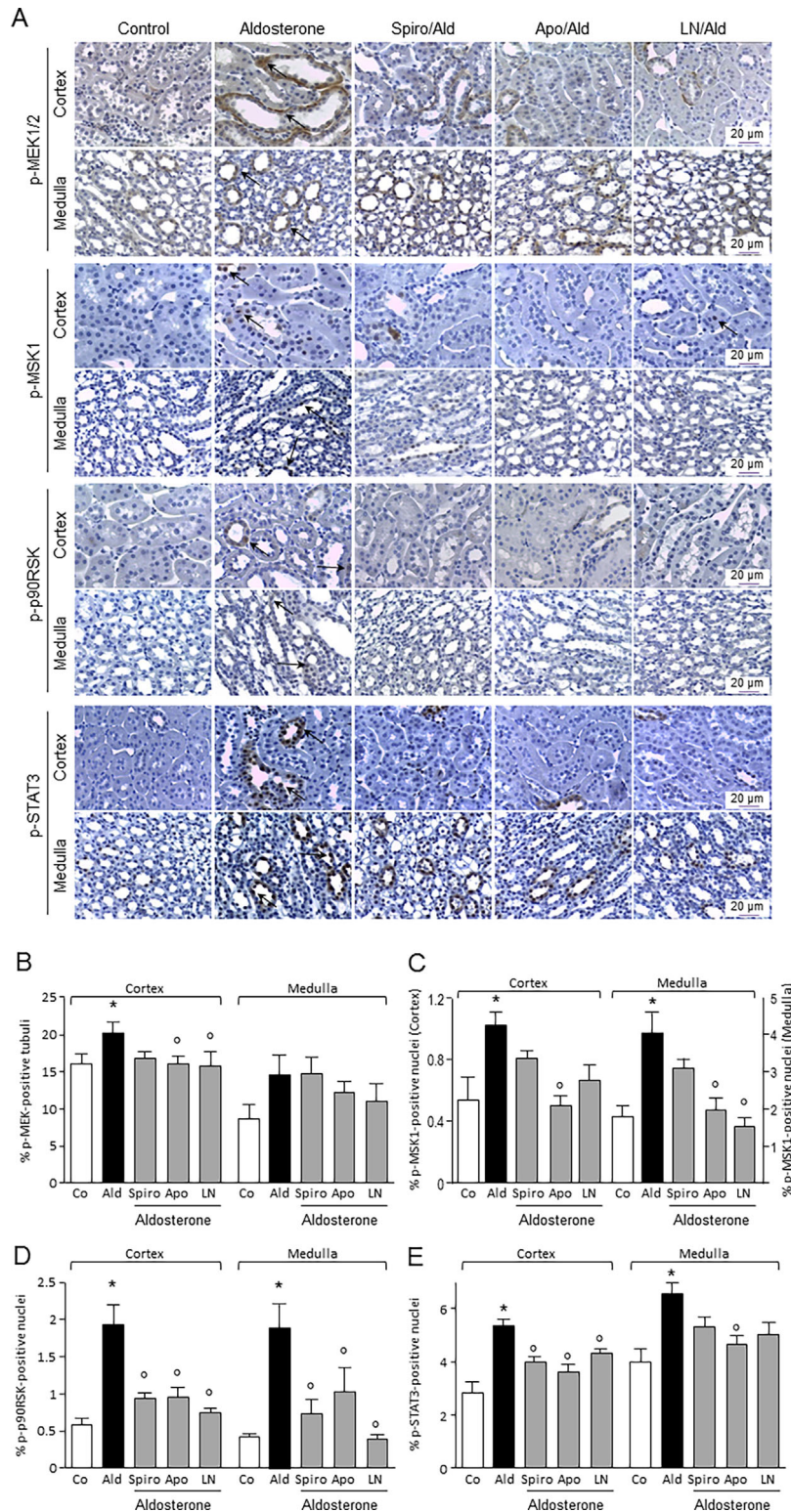
FIGURE 8 Ald activates upstream and downstream events of the ERK1/2 signaling pathway in vivo. Rats were untreated (Control; Co) or treated for 4 weeks with aldosterone (Ald), and simultaneously with spironolactone (Spiro), apocynin (Apo), or L-NAME (LN). (A) Representative images for the IHC staining of phospho-(Ser217/221)-MEK1/2-positive tubules, phospho-(Thr581)-MSK1-positive nuclei, phospho-(Ser380)-p90RSK-positive nuclei, and phospho-(Ser727)-STAT3-positive nuclei from cortex and medulla are shown. Arrows highlight positive cells. (B-E) Quantification of p(Ser217/221)-MEK1/2-positive tubules (B), p(Thr581)-MSK1-positive nuclei (C), p(Ser380)-p90RSK-positive nuclei (D), and p(Ser727)-STAT3-positive nuclei (E) was done using the cell image analysis software CellProfiler[33] within eight visual fields. Results are shown as mean ± SEM. *$P \leq 0.05$ versus control, °$P \leq 0.05$ versus Ald treatment
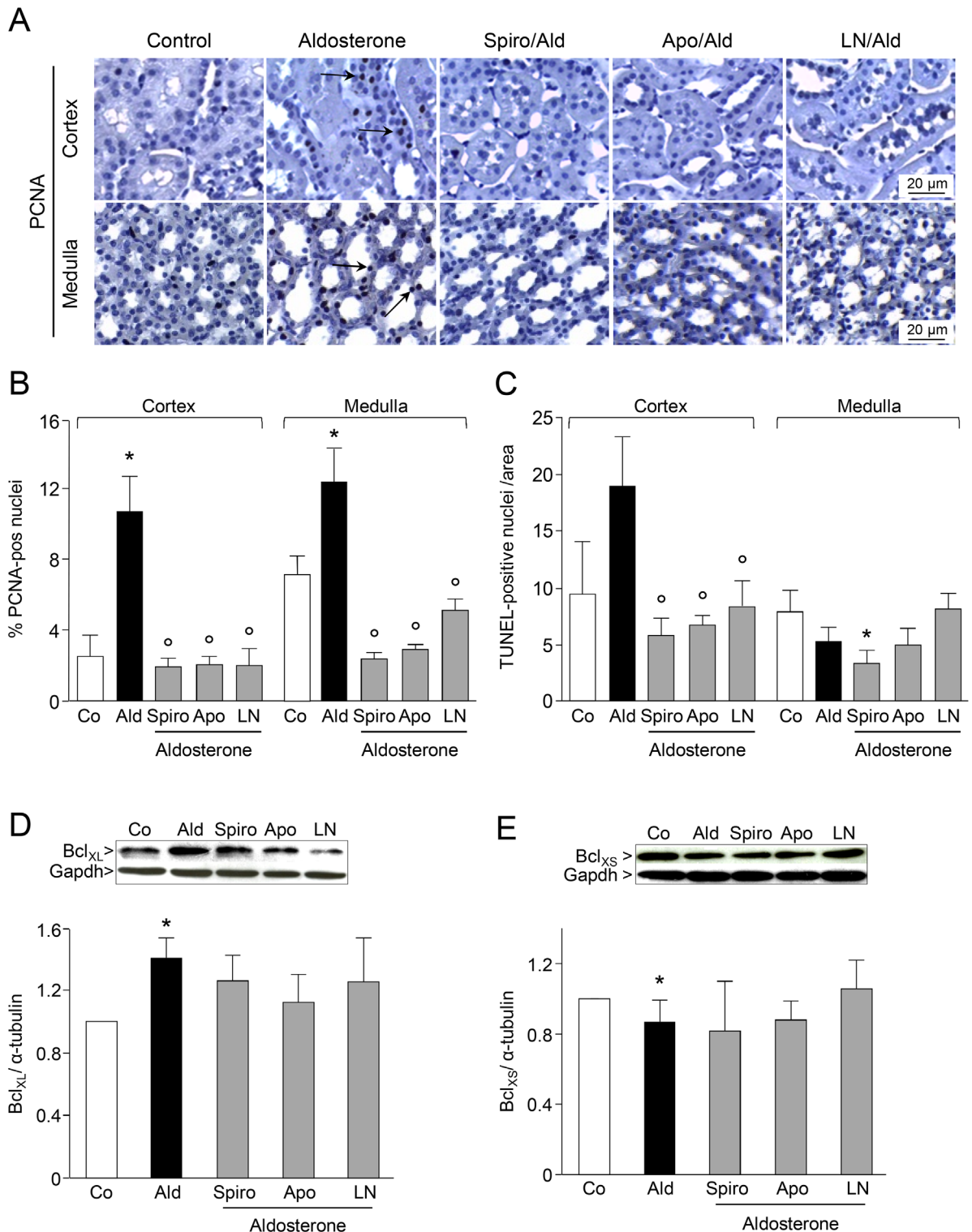
FIGURE 9   Ald-mediated activation of ERK1/2 and STAT3 leads to increased cell proliferation and reduced apoptosis in vivo. Rats were untreated (Control; Co) or treated for 4 weeks with aldosterone (Ald), and simultaneously with spironolactone (Spiro), apocynin (Apo), or L-NAME (LN). (A) Representative images for the IHC staining of PCNA-positive nuclei from cortex and medulla are shown. Arrows highlight positive cells. (B) PCNA-positive cells quantified with the cell image analysis software CellProfiler[33] within at least eight visual fields. (C) Amount of apoptotic cells determined with the TUNEL assay within 3-6 visual fields. (D and E) The expression of the anti-apoptotic Bcl_{XL} (D) and the pro-apoptotic Bcl_{XS} (E) was measured by Western blot in kidney extracts. Representative images and the quantification of the bands are shown. Results are shown as mean ± SEM. *$P \leq 0.05$ versus control, °$P \leq 0.05$ versus Ald treatment

fibroblasts and kidney cells.[36–39] Once activated, ERK1/2 primarily phosphorylates a large number of target substrates on serine or threonine residues followed by a proline residue.[40] Given that the cell cycle regulatory proteins that are activated by ERK1/2 are localized in the nucleus, access of ERK1/2 to its substrates is essential for their regulation. Accordingly we observed that Ald promotes the activation of ERK1/2 and their nuclear substrates p90RSK, MSK1 and STAT3 in kidney tubular cells. In response to angiotensin II, STAT1 and STAT2 are rapidly tyrosine-phosphorylated in rat aortic smooth muscle cells,[41] however no studies concerning the capacity of Ald to activate STAT proteins exist. A constitutive activation of STAT3 is frequently observed in different types of cancer. Although STAT3 does not match the classical oncogen definition, it is a powerful activator of malignant transformation controling the expression of target genes that regulate cell proliferation and survival.[42] STAT3 is responsible for the expression of anti-apoptotic genes, which is in line with our results both in vitro and in vivo, and for the survival of premalignant cells harboring mutations, which make these cells resistant against genotoxic insults.[43]

The Ras/Raf/MEK/ERK pathway can be silenced by MEK1/2 inhibitors,[44] which is an important approach in the treatment of cancers like renal cell carcinomas.[45] ERK, and in particular ERK2, is regarded as the bona fide STAT3 serine kinase.[46] Supporting the concept that STAT3 is activated by Ald via ERK1/2, MEK chemical inhibition prevented Ald-induced ERK1/2 activation and the subsequent Ser727 phosphorylation and nuclear localization of STAT3. Although the initial activation event in the STAT3 cascade is the phosphorylation in Tyr705, Ser727 phosphorylation is required for maximal STAT3 transcriptional activity. Ser727 phosphorylation is important in the survival of distinct cell types,[47] and in postnatal survival and growth of mice.[48] Accordingly, we observed that in kidney cells the increased STAT3 phosphorylation is associated with an increased expression of the STAT3-regulated prosurvival gene Bcl$_{XL}$.

Ald-induced activation of ERK1/2 and STAT3 was mediated via the MR, which was evidenced by the in vivo and in vitro inhibitory capacity of MR antagonists. MR antagonists were previously shown to also block Ald-induced activation of ERK1/2 in vascular smooth muscle cells and in rat kidneys.[49,50] These and our data are inconsistent with other findings showing that the effects of Ald on ERK1/2 activity were insensitive to the classical MR antagonists in cortical collecting duct cells.[51] This discrepancy could be due to differences in experimental conditions, cell types or time points studied. In this regard, while Rossol-Haseroth et al investigated rapid, non-genomic Ald effects, we analyzed the genomic effects of Ald.[51] Very importantly, our current work shows for the first time the occurrence of interactions between the mineralocorticoid receptor and the STAT3 pathway.

We previously reported that excess Ald causes in kidney tubular cells the activation of NADPH oxidase and NO synthase leading to an increased production of superoxide anion and NO.[2,3,5,6,52] We currently observed that this high production of reactive oxygen and nitrogen species underlies in part the activation of the ERK1/2 pathway, and downstream of STAT3. This is supported by findings that the chemical inhibition of NADPH oxidase and NO synthase both in vitro and in vivo, prevents the activation by Ald of ERK1/2 and STAT3 in LLC-PK1 cells and in the rat renal cortex. Ald/NAD(P)H oxidase-mediated activation of ERK, and consequently of STAT3, can occur through several mechanisms including: i) the oxidation-dependent inhibition of intracellular tyrosine phosphatases; and ii) oxidants-mediated expression and activation of the small Rac protein upstream of ERK.[53] In fact, the NAD(P)H oxidase-dependent activation of STAT3 by angiotensin II was described in rat aortic smooth muscle cells.[54] The link among NO synthase activation, increased NO production, ERK1/2 activation, and cancer has been previously described. For example, pretreatment of human astrocytoma cells with the NO synthase inhibitor L-NAME antagonized ERK1/2 leading to reduced cell proliferation.[55] In line with these findings, we currently observed both in vitro and in vivo, that L-NAME significantly reduced Ald-induced ERK1/2 activation in kidney cells.

In agreement with our previous findings[5] and with the roles of ERK1/2 and STAT3 on cell proliferation and survival, Ald caused an increase in cell proliferation both in vitro and in vivo. Increased cell proliferation was previously detected in kidneys from DOCA/salt-treated rats, mainly in the tubular regions.[56] Enhanced cell proliferation is also found in the brain from DOCA/salt-treated rats.[57] All intervention groups studied in vivo (Ald plus inhibitors of the MR, NADPH oxidase and NOS) showed significantly lower rates of PCNA-positive nuclei in cortex compared to Ald-treated animals. These results indicate both the involvement of the MR, and the requirement of elevated superoxide and NO production in the triggering of ERK1/2/STAT3-mediated increased cell proliferation.

Survival of all somatic cells requires the continuous input of survival signals to suppress apoptosis. We observed that, overall, excess Ald had antiapoptotic actions as indicated by: i) upregulation of the antiapoptotic protein Bcl$_{XL}$; ii) downregulation of proapoptotic proteins, i.e. Bcl$_{XS}$; Bak; iii) decreased apoptotic rates in LLC-PK1 cells. Results obtained in vivo did not show significant differences, which stresses the need for future studies to distinguish specific effects on proximal and distal tubular cells. Furthermore, the effects on cell proliferation could be the early and most important effects of hyperaldosteronism or maybe longer periods of exposure to high Ald levels could be required to observe an effect on apoptosis.

In summary, this work showed that exposure to high Ald concentrations leads to the activation of the Raf/MEK/ERK pathway and downstream of the prosurvival transcription factor STAT3 in kidney cells both in vitro and in vivo. This is in part mediated by the Ald-induced activation of NADPH oxidase and NOS, and the associated production of superoxide anion and NO. As a consequence of ERK1/2/STAT activation, Ald caused increased cell proliferation and resistance to apoptosis in kidney cells, with a mild effect observed in rat kidney medulla. Thus, the aberrant and long-term activation of STAT3 via ERK1/2 by persistently high Ald levels could unfold a prosurvival/proliferative signaling shift in kidney cells, leading to the survival of cells with damaged DNA, and therefore increase the risk for the genesis of mutated cells. These results contribute to the understanding of the mechanisms underlying the adverse effects of hyperaldosteronism in the kidney. Importantly, they strongly support

the concept that Ald might indeed play a so far undescribed but important role in the increased kidney cancer risk observed in hypertensive patients.

REFERENCES

1. Skott O, Uhrenholt TR, Schjerning J, Hansen PB, Rasmussen LE, Jensen BL. Rapid actions of aldosterone in vascular health and disease-friend or foe? *Pharmacol Ther*. 2006;111:495–507.

2. Queisser N, Oteiza PI, Stopper H, Oli RG, Schupp N. Aldosterone induces oxidative stress, oxidative DNA damage and NF-kappaB-activation in kidney tubule cells. *Mol Carcinog*. 2011;50:123–135.

3. Schupp N, Queisser N, Wolf M, et al. Aldosterone causes DNA strand breaks and chromosomal damage in renal cells, which are prevented by mineralocorticoid receptor antagonists. *Horm Metab Res*. 2010; 42:458–465.

4. Queisser N, Happ K, Link S, et al. Aldosterone induces fibrosis, oxidative stress and DNA damage in livers of male rats independent of blood pressure changes. *Toxicol Appl Pharmacol*. 2014;280:399–407.

5. Queisser N, Amann K, Hey V, Habib SL, Schupp N. Blood pressure has only minor influence on aldosterone-induced oxidative stress and DNA damage in vivo. *Free Radic Biol Med*. 2013;54:17–25.

6. Queisser N, Oteiza PI, Link S, Hey V, Stopper H, Schupp N. Aldosterone activates transcription factor Nrf2 in kidney cells both in vitro and in vivo. *Antioxid Redox Signal*. 2014;21:2126–2142.

7. Friis S, Sorensen HT, Mellemkjaer L, et al. Angiotensin-converting enzyme inhibitors and the risk of cancer: a population-based cohort study in Denmark. *Cancer*. 2001;92:2462–2470.

8. Moore LE, Wilson RT, Campleman SL. Lifestyle factors, exposures, genetic susceptibility, and renal cell cancer risk: a review. *Cancer Invest*. 2005;23:240–255.

9. Ljungberg B, Campbell SC, Choi HY, et al. The epidemiology of renal cell carcinoma. *Eur Urol*. 2011;60:615–621.

10. Weikert S, Boeing H, Pischon T, et al. Blood pressure and risk of renal cell carcinoma in the European prospective investigation into cancer and nutrition. *Am J Epidemiol*. 2008;167:438–446.

11. Lang K, Weber K, Quinkler M, et al. Prevalence of malignancies in patients with primary aldosteronism. *J Clin Endocrinol Metab*. 2016; 101:1656–1663.

12. Huang LL, Nikolic-Paterson DJ, Ma FY, Tesch GH. Aldosterone induces kidney fibroblast proliferation via activation of growth factor receptors and PI3K/MAPK signalling. *Nephron Exp Nephrol*. 2012;120:e115–e122.

13. Brem AS, Gong R. Therapeutic targeting of aldosterone: a novel approach to the treatment of glomerular disease. *Clin Sci (Lond)*. 2015; 128:527–535.

14. Roskoski R, Jr. ERK1/2 MAP kinases: structure, function, and regulation. *Pharmacol Res*. 2012;66:105–143.

15. Schaeffer HJ, Weber MJ. Mitogen-activated protein kinases: specific messages from ubiquitous messengers. *Mol Cell Biol*. 1999; 19: 2435–2444.

16. Morrison DK, Cutler RE. The complexity of Raf-1 regulation. *Curr Opin Cell Biol*. 1997;9:174–179.

17. Seger R, Ahn NG, Posada J, et al. Purification and characterization of mitogen-activated protein kinase activator(s) from epidermal growth factor-stimulated A431 cells. *J Biol Chem*. 1992;267:14373–14381.

18. Lewis TS, Shapiro PS, Ahn NG. Signal transduction through MAP kinase cascades. *Adv Cancer Res*. 1998;74:49–139.

19. Wong KK. Recent developments in anti-cancer agents targeting the Ras/Raf/ MEK/ERK pathway. *Recent Pat Anticancer Drug Discov*. 2009;4:28–35.

20. Mansour SJ, Matten WT, Hermann AS, et al. Transformation of mammalian cells by constitutively active MAP kinase kinase. *Science*. 1994;265:966–970.

21. Bromberg J, Chen X. STAT proteins: signal tranducers and activators of transcription. *Methods Enzymol*. 2001;333:138–151.

22. Timofeeva OA, Plisov S, Evseev AA, et al. Serine-phosphorylated STAT1 is a prosurvival factor in Wilms' tumor pathogenesis. *Oncogene*. 2006;25:7555–7564.

23. McCubrey JA, May WS, Duronio V, Mufson A. Serine/threonine phosphorylation in cytokine signal transduction. *Leukemia*. 2000;14:9–21.

24. Calo V, Migliavacca M, Bazan V, et al. STAT proteins: from normal control of cellular events to tumorigenesis. *J Cell Physiol*. 2003; 197:157–168.

25. Guo C, Yang G, Khun K, et al. Activation of Stat3 in renal tumors. *Am J Transl Res*. 2009;1:283–290.

26. Horiguchi A, Asano T, Kuroda K, et al. STAT3 inhibitor WP1066 as a novel therapeutic agent for renal cell carcinoma. *Br J Cancer*. 2010; 102:1592–1599.

27. Hui Z, Tretiakova M, Zhang Z, et al. Radiosensitization by inhibiting STAT1 in renal cell carcinoma. *Int. J Radiat Oncol Biol Phys*. 2009;73:288–295.

28. Bowman T, Garcia R, Turkson J, Jove R. STATs in oncogenesis. *Oncogene*. 2000;19:2474–2488.

29. Mackenzie GG, Zago MP, Keen CL, Oteiza PI. Low intracellular zinc impairs the translocation of activated NF-kappa B to the nuclei in human neuroblastoma IMR-32 cells. *J Biol Chem*. 2002; 277: 34610–34617.

30. Bradford MM. A rapid and sensitive method for the quantitation of microgram quantities of protein utilizing the principle of protein-dye binding. *Anal Biochem*. 1976;72:248–254.

31. Rasband WS. Image J Software Program. U.S. National Institute of Health, Bethesda (MD). 1997-2008.

32. Mackenzie GG, Queisser N, Wolfson ML, Fraga CG, Adamo AM, Oteiza PI. Curcumin induces cell-arrest and apoptosis in association with the inhibition of constitutively active NF-κB and STAT3 pathways in Hodgkin's lymphoma cells. *Int J Cancer*. 2008;123:56–65.

33. Lamprecht MR, Sabatini DM, Carpenter AE. CellProfiler: free, versatile software for automated biological image analysis. *Biotechniques*. 2007;42:71–75.

34. Krüger K, Ziegler V, Hartmann C, et al. Lovastatin prevents cisplatin-induced activation of pro-apoptotic DNA damage response (DDR) of renal tubular epithelial cells. *Toxicol Appl Pharmacol*. 2016; 292:103–114.

35. Hilger RA, Scheulen ME, Strumberg D. The Ras-Raf-MEK-ERK pathway in the treatment of cancer. *Onkologie*. 2002;25:511–518.

36. Terada Y, Kobayashi T, Kuwana H, et al. Aldosterone stimulates proliferation of mesangial cells by activating mitogen-activated protein kinase 1/2, cyclin D1, and cyclin A. *J Am Soc Nephrol*. 2005;16:2296–2305.

37. Huang S, Zhang A, Ding G, Chen R. Aldosterone-induced mesangial cell proliferation is mediated by EGF receptor transactivation. *Am J Physiol*. 2009;296:F1323–F1333.

38. Manegold JC, Falkenstein E, Wehling M, Christ M. Rapid aldosterone effects on tyrosine phosphorylation in vascular smooth muscle cells. *Cell Mol Biol (Noisy-le-Grand)*. 1999;45:805–813.

39. Stockand JD, Meszaros JG. Aldosterone stimulates proliferation of cardiac fibroblasts by activating Ki-RasA and MAPK1/2 signaling. *Am J Physiol Heart Circ Physiol*. 2003;284:H176–H184.

40. Mebratu Y, Tesfaigzi Y. How ERK1/2 activation controls cell proliferation and cell death: is subcellular localization the answer? *ABBV Cell Cycle*. 2009;8:1168–1175.

41. Marrero MB, Schieffer B, Paxton WG, et al. Direct stimulation of Jak/STAT pathway by the angiotensin II AT1 receptor. *Nature*. 1995;375:247–250.

42. Atkinson GP, Nozell SE, Benveniste ET. NF-kappaB and STAT3 signaling in glioma: targets for future therapies. *Expert Rev Neurother*. 2010;10:575–586.

43. Grivennikov SI, Karin M. Dangerous liaisons: STAT3 and NF-kappaB collaboration and crosstalk in cancer. *Cytokine Growth Factor Rev*. 2010;21:11–19.

44. McCubrey JA, Steelman LS, Abrams SL, et al. Emerging MEK inhibitors. *Expert Opin Emerg Drugs*. 2010;15:203–223.

45. Stadler WM. Targeted agents for the treatment of advanced renal cell carcinoma. *Cancer*. 2005;104:2323–2333.

46. Decker T, Kovarik P. Serine phosphorylation of STATs. *Oncogene*. 2000;19:2628–2637.

47. Liu H, Ma Y, Cole SM, et al. Serine phosphorylation of STAT3 is essential for Mcl-1 expression and macrophage survival. *Blood*. 2003;102:344–352.

48. Shen Y, Schlessinger K, Zhu X, et al. Essential role of STAT3 in postnatal survival and growth revealed by mice lacking STAT3 serine 727 phosphorylation. *Mol Cell Biol*. 2004;24:407–419.

49. Ishizawa K, Izawa Y, Ito H, et al. Aldosterone stimulates vascular smooth muscle cell proliferation via big mitogen-activated protein kinase 1 activation. *Hypertension*. 2005;46:1046–1052.

50. Nishiyama A, Yao L, Nagai Y, et al. Possible contributions of reactive oxygen species and mitogen-activated protein kinase to renal injury in aldosterone/salt-induced hypertensive rats. *Hypertension*. 2004;43:841–848.

51. Rossol-Haseroth K, Zhou Q, Braun S, et al. Mineralocorticoid receptor antagonists do not block rapid ERK activation by aldosterone. *Biochem Biophys Res Commun*. 2004;318:281–288.

52. Queisser N, Schupp N, Stopper H, Schinzel R, Oteiza PI. Aldosterone increases kidney tubule cell oxidants through calcium-mediated activation of NADPH oxidase and nitric oxide synthase. *Free Radic Biol Med*. 2011;51:1996–2006.

53. Go YM, Gipp JJ, Mulcahy RT, Jones DP. H2O2-dependent activation of GCLC-ARE4 reporter occurs by mitogen-activated protein kinase pathways without oxidation of cellular glutathione or thioredoxin-1. *J Biol Chem*. 2004;279:5837–5845.

54. Schieffer B, Luchtefeld M, Braun S, Hilfiker A, Hilfiker-Kleiner D, Drexler H. Role of NAD(P)H oxidase in angiotensin II-induced JAK/STAT signaling and cytokine induction. *Circ Res*. 2000;87:1195–1201.

55. Meini A, Sticozzi C, Massai L, Palmi M. A nitric oxide/Ca(2+)/calmodulin/ERK1/2 mitogen-activated protein kinase pathway is involved in the mitogenic effect of IL-1beta in human astrocytoma cells. *Br J Pharmacol*. 2008;153:1706–1717.

56. Schupp N, Kolkhof P, Queisser N, et al. Mineralocorticoid receptor-mediated DNA damage in kidneys of DOCA-salt hypertensive rats. *FASEB J*. 2011;25:968–978.

57. Pietranera L, Saravia FE, Roig P, Lima A, De Nicola AF. Protective effects of estradiol in the brain of rats with genetic or mineralocorticoid-induced hypertension. *Psychoneuroendocrinology*. 2008;33:270–281.